

The Role of the Gas Pressure on the Foaming of Metals Following the PM-route

Francisco Garcia-Moreno^{1,2}, Norbert Babcsan^{1,2}, John Banhart^{1,2}

¹ Hahn-Meitner Institute, Glienicke Strasse 100, 14109 Berlin, Germany

² Technical University, Hardenbergstrasse 36, 10623 Berlin, Germany

Metal foaming is investigated under different surrounding air gas pressures. The experimental setup consists of a microfocus X-ray source, a X-ray transparent foaming heater and a flat panel detector. With a special pressurised foaming heater in-situ and real-time X-ray radioscopic observation of the process varying the gas pressure is possible. Using an image analysis software foam expansion and coalescence can be determined quantitatively from the radioscopic images. Ex-situ 2D foam structure analysis gives us additional information about pore size diameters, pore size distribution and pore roundness. Foaming under pressure shows that expansion, coalescence and pore size are reduced, and that foam stability and pore roundness are increased. All these parameters are closely related to each other, but the pore size dependence is not as expected from an ideal gas. It rather is a combination of several mechanisms including coalescence and pressure-dependent blowing agent decomposition. Controlling gas pressure we are able to adjust pore size or foam density simply and precisely, which could be very important from the engineering point of view.

Keywords: metallic foam, gas pressure, pore size diameter, X-ray radioscopic

1. Introduction

In the past a lot of effort was put into controlling the pore size and pore size uniformity of metal foams produced by the powder metallurgical route¹. Variations of foaming parameters such as blowing agent content^{2,3}, temperature profile⁴, etc. allow for an adjustment of density, expansion and pore size only within a restricted range since these properties are closely connected to each other and are difficult to control independently. As the gas production kinetics of the blowing agent is very sensitive to temperature variations, well defined and reproducible foaming conditions are necessary but often hard to achieve. From the application point of view reproducibility and well defined properties are essential parameters for successful commercialisation. The lack of control of these may be, together with the still too high production costs, the most important reason for the slow market penetration of metallic foams in the past years.

It is known that pressure has a pronounced effect on metal foaming^{5,6}. However, the study of pressure effects is experimentally challenging. The combination of an in-situ X-ray scanner and a pressurised furnace allowed us to investigate the pressure effect and to show that the ambient gas pressure p is a very important parameter for the control of metal foam structure.

2. Experimental procedure

Pure Al, Si and Cu powders were mixed with 0.5 wt% TiH₂ powder and subsequently hot-compacted uni-axially for 5 minutes at 400°C and under a pressure of 300 MPa to cylindrical ($\varnothing = 36$ mm) AlSi6Cu4-alloy foamable precursors.

A 150 kV microfocus X-ray source with 5 μ m spot size and a 2240 x 2368 pixels panel detector with 50 μ m pixel size, both from Hamamatsu, were used for real-time radioscopic. The adjustable geometrical magnification due to the cone beam geometry was set to 4 times, the image acquisition rate was 1 Hz. To allow for radioscopic in-situ investigations of the influence of the ambient gas pressure on foaming behaviour, a X-ray transparent pressure furnace built especially for this purpose was utilised (see fig. 1). It consists of an Al-tube ($\varnothing_{\text{out}} = 40$ mm, $l =$

200 mm, $d = 0.5$ mm) that can be hermetically sealed at both ends and is thin enough for X-ray transparency. The gas type and pressure inside can be regulated through gas in- and outlets on one side. On the other side is a lead-through with electrical connectors for a thermocouple and for a resistive heating plate installed inside with a power of 500 W. This can provide heating rates up to 35 K/s and a maximum temperature of 800 °C. The furnace was tested successfully in the pressure range of $p = 0.01$ bar to 10 bar. The furnace⁴ and the radioscopic set-up⁷ are explained in more detail elsewhere.

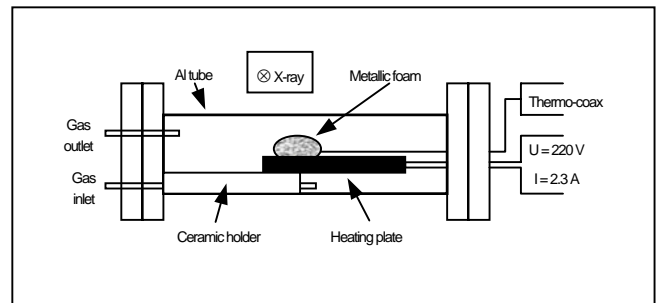


Fig. 1 Draft view of the X-ray transparent foaming pressure furnace.

All specimens for a series of measurements under varying air pressures were prepared from the same uni-axially pressed precursor tablet to avoid possible discrepancies coming from different compaction conditions. Samples of 8x8x2 mm³ size were prepared to fit in the pressure furnace. The samples were heated up for around 30 s at a constant heating rate of 20 K/s to the final temperature of 600°C and then held at this temperature for further 90 s (see fig. 3).

The series of X-ray images of the foaming process gives an accurate description of foam expansion kinetics and foam structure development. With help of "AXIM", a self developed X-ray images analysis software described elsewhere⁸, quantitative analysis of foam properties such as 2D expansion perpendicular to the X-ray beam F/F_0 , foam density, drainage or

coalescence rate can be extracted from the sequences of radioscopic images.

2D pore size analysis from the solidified foams was performed by mechanical cutting of the samples and polishing. After increasing the contrast between pores and cell walls using graphite powder spray followed by a second grinding step of the cell walls with P2500 sandpaper, the samples were scanned with a normal flat scanner. The resulting images were binarised, adjusting the contrast that way, after which the pores become black and the cell walls white. With the image analysis software "Image Tool"[®]) an automatic pore detection can be performed, achieving quantitative 2D data of pore size, mean Feret diameter $\sqrt{(4 \times \text{area} / \pi)}$ and mean pore roundness $(4 \times \pi \times \text{area}) / \text{perimeter}$. A circle will have a roundness of 1.

3. Results

3.1 Foaming kinetics

The first impression that we gain from the X-ray image series of foams made under different gas pressures is, that foaming with the highest gas pressures results in a reduced *maximal expansion*. In fig. 2 we can see X-ray radiograms of samples foamed under different gas pressures 120 s after starting heating. Clearly, for $p \geq 7$ bar the resulting foam is smaller. Also we can see that the *pore size* gets smaller with increasing pressure beyond $p \geq 5$ bar. Finally we find that the *pore size distributions* appear more uniform for foams made under higher pressures.

Looking at the sequence of images we observe that at the high pressure levels less *cell wall ruptures* are observed, corresponding to a higher foam stability. Moreover, less collapse between the end of heating and foam solidification occurs for high pressures.

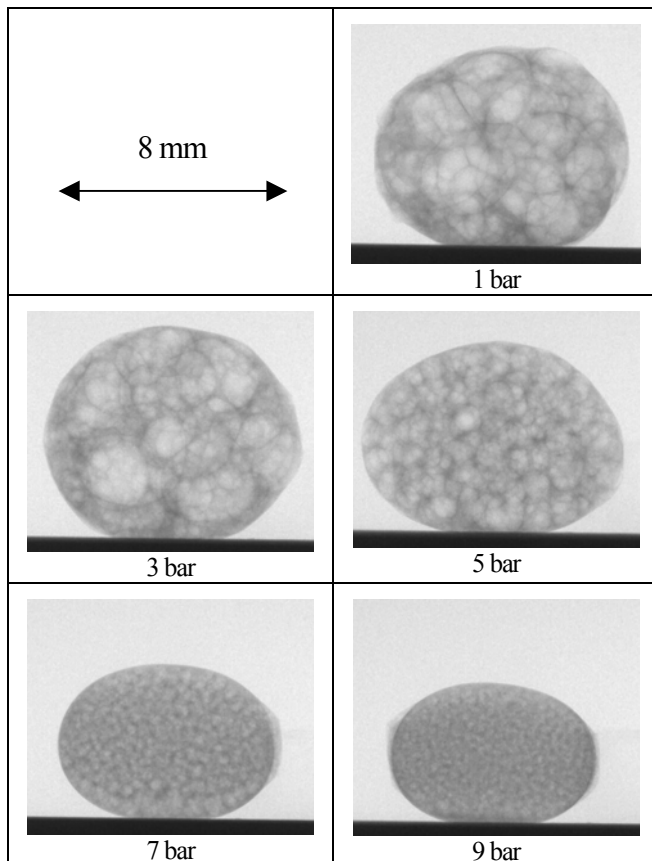


Fig. 2 X-ray radiograms of AlSi6Cu4-foams in the liquid state for different gas pressures ($t = 120$ s after starting heating).

3.2 Foam expansion

After a first qualitative description we quantified the results using the image analysis software "AXIM". Fig. 3 shows the expansion courses of the various foams for pressures $1 \text{ bar} \leq p \leq 9 \text{ bar}$. We can also see a temperature profile representative for all the samples. It shows three regimes: a fast heating ramp up to $\sim 600^\circ\text{C}$ at 20 K/s, a holding period at this temperature up to 120s after starting heating and a cooling stage after the end of heating. The undulations at 600°C are caused by the PID controller and are caused by the small heat capacity of our small samples.

About 25 s after starting heating the samples begin to foam. The main expansion is completed after 50 s. 120 s after starting heating cooling begins and the samples contract considerably until reaching the solidification point after around 150-160 s. The sample foamed under 3 bar has the largest expansion as long as the foams are still in the liquid state. After solidification the foam made under 5 bar shows the largest expansion. In this case the foam made under 5 bar was more stable than the foam made under 3 bar.

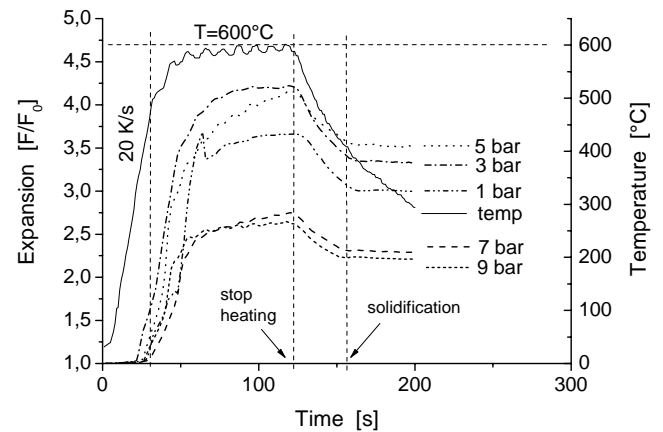


Fig. 3 Expansion behaviour expressed by the increase in foam area of AlSi6Cu4 specimens foamed under different surrounding pressures. Temperature profile representative for all the foaming experiments, with 3 steps: heating ramp with 20K/s, holding up to 120 s at 600°C and cooling.

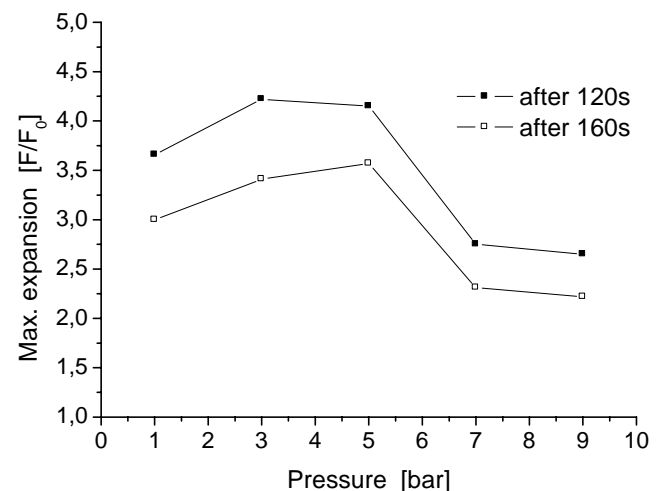


Fig. 4 Maximum expansion of AlSi6Cu4 specimens foamed under different surrounding pressures after 120 s and 160 s corresponding to fig. 3.

If we plot the expansion after 120 s as a function of pressure (fig. 4) we can clearly observe a maximum at around 3 to 4 bar. For values corresponding to the end of expansion after 160 s this maximum still exists, but is shifted to about 4 to 5 bar. The reason for the shift of the maximum after 160 s is the increased contraction of the foams under lower pressures during solidification.

3.3 Foam coalescence

In order to obtain a quantitative measure for foam stability the cumulated number of cell wall rupture events starting from the fully expanded foam ($t \cong 50$ s) and ending at the solidification point ($t \cong 160$ s) were counted with AXIM and plotted in fig. 5.

We can see a clear pressure dependence of the number of cell wall ruptures, namely a decrease of the ruptures with increasing pressure. This curve corroborates the behaviour observed qualitatively in the radioscopic images and in the cross sections, where for high pressures more stable pores could be observed.

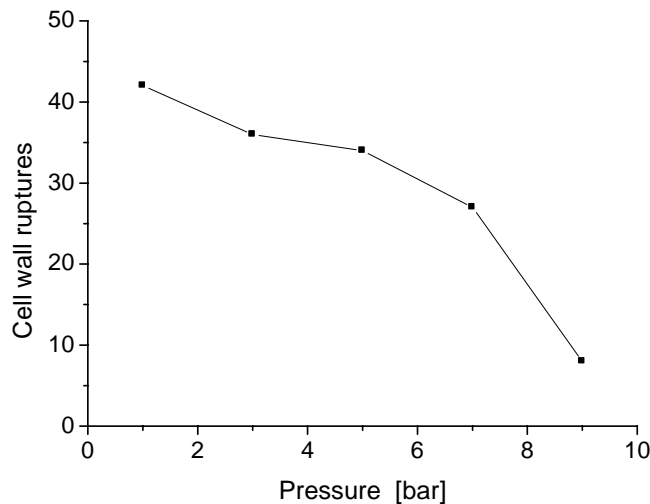


Fig. 5 Coalescence strength quantified by the cumulated number of cell wall ruptures in the fully expanded specimens. Ruptures correspond to experiments in fig. 3 between 50 s and 160 s after the start of heating.

3.3 Pore structure

To determine the pore size, cross sections of the metallic foams were prepared (fig. 6). The samples correspond to the foams in fig. 2, 3 and 4 after solidification ($t > 200$ s). Here we can see for 5, 7 and 9 bar very small pores with a relative homogeneous pore size distribution. No significant drainage is observed. For 1 and 3 bar we have metal foams with big and small pores, with increased drainage and collapsed pores. This was also observed in the radioscopic image sequences.

Of great interest is the mean pore size diameter as a function of pressure (fig. 7). It decreases for increasing pressure with a more or less linear decay up to 7 bar. The standard deviation is high for low pressures because of the low number of pores in our small samples which do not allow for good statistics. The standard deviation decreases with pressure not only because of the higher number of pores but also because of increasing homogeneity of

the foam. In the images in fig. 6 we can observe clearly this increasing homogeneity from 1 to 9 bar.

If we plot the maximal pore diameter against pressure we can see a similar behaviour as for the mean diameter, with also a relatively linear diameter reduction from 1 to 7 bar.

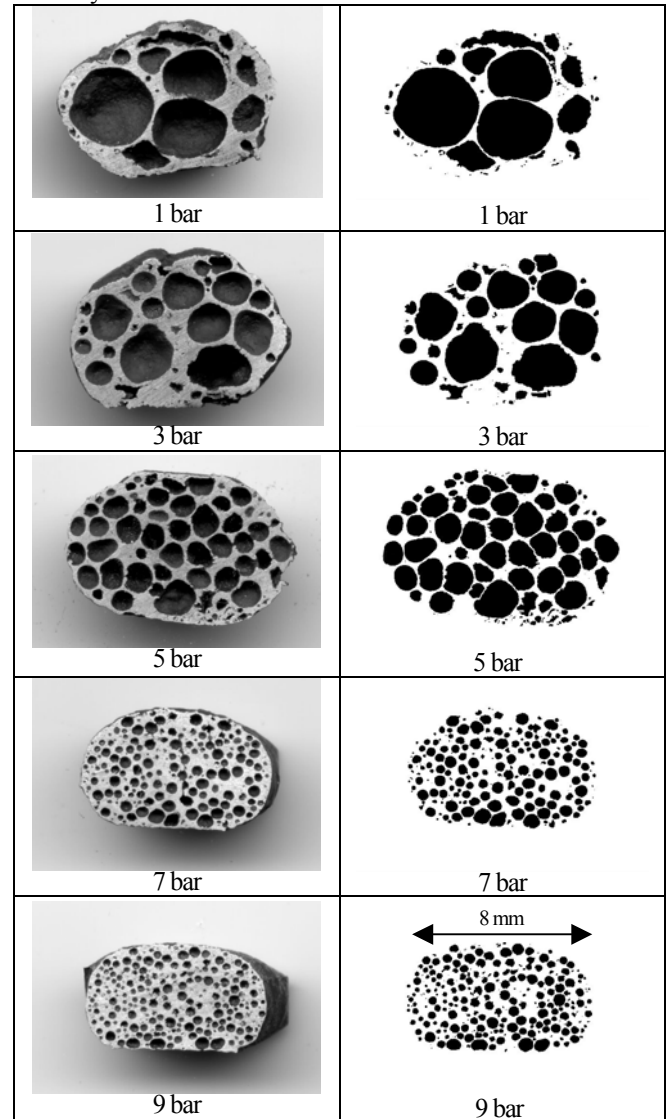


Fig. 6 2D pore structure of AlSi6Cu4 samples foamed at different pressures. Optical scanned images (left) and binarised images (right). ($t > 200$ s).

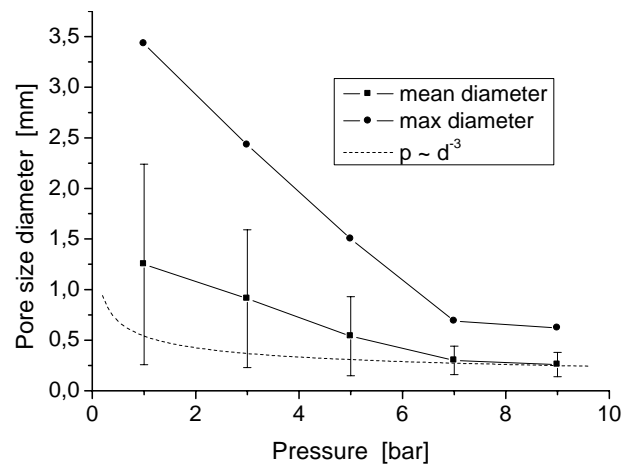


Fig. 7 Mean, maximum and expected pore diameter in dependence of gas pressure. Samples corresponding to fig. 6.

The pore roundness for the samples in fig. 6 is shown in fig. 8. It increases with pressure and seems to have a maximum at $p = 7$ to 8 bar. This effect can be understood as at high pressures the mean pore diameter and the expansion decreases. Hence, the density is higher, the cell walls are thicker and the pores are still small so that they don't disturb each other to reach the ideal round form. They still don't "touch" each other, as we can see in fig. 9.

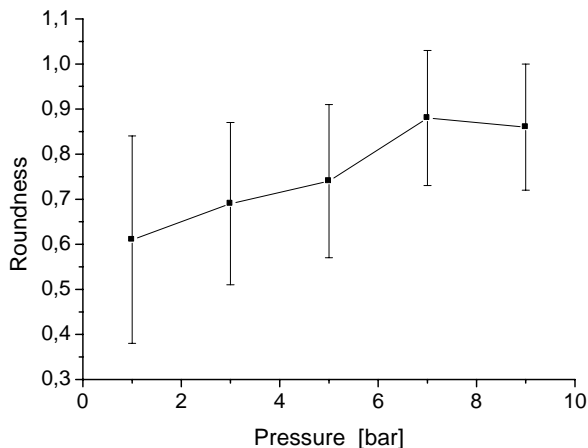


Fig. 8 Pore roundness in dependence of gas pressure. Samples corresponding to fig. 6.

Of course this result is for a given alloy at a given temperature. Data are different for other foaming temperatures. Especially the pore diameter (fig. 9) and the expansion^{4,10} are expected to be temperature sensitive.

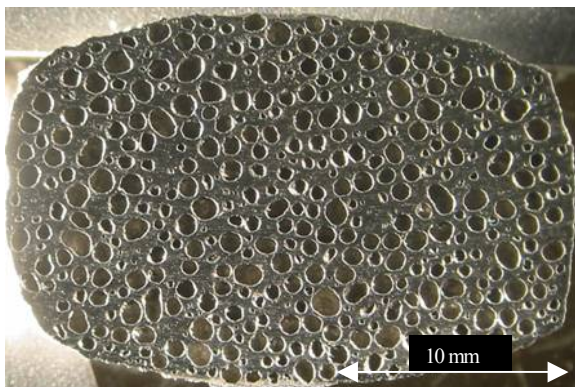


Fig. 9 Pore structure of a fully expanded AlSi6Cu4 sample foamed at $T = 630^\circ\text{C}$ and 9 bar. A homogenous distribution of small and round pores can be observed. Mean pore diameter ($d_{T=630^\circ\text{C}} = 0.55 \pm 0.19$ mm) is larger than for $T = 600^\circ\text{C}$ ($d_{T=600^\circ\text{C}} = 0.26 \pm 0.12$ mm), compare to fig. 6.

4. Discussion

In order to understand some of the pressure dependencies observed it is useful to first consider an ideal foam. In this foam the gas release by the blowing agent depends on temperature only, not on pressure. The gas solubility in the liquid is assumed to be zero. Moreover, once bubbles are blown the films between adjacent bubbles remain stable, i.e. there is no coalescence. In such a foam one would expect that the bubble volume is inversely proportional to the external pressure p , as $V = nRT/p$. For the

diameter one would therefore expect $d \propto p^{-1/3}$. In fig. 7 this function is shown. Obviously the decrease in bubble size with increasing pressure is so much stronger that the compression of the gas in the cells cannot serve as the only explanation.

One possible reason for the discrepancy is that the mole number n is not constant. A higher counter pressure of hydrogen in the cells surrounding the decomposing the blowing agent particles would retard decomposition, or, going from high to low pressures, there would be more gas available and pores would be larger.

The solubility of hydrogen is another possible reason. At high pressures more hydrogen is dissolved in the liquid metal and cannot contribute to bubble inflation. According to Sievert's law the concentration of gas dissolved in the melt is $c \sim e^{(-1/kT)} \times p^{1/2}$. However, for a pressure difference of $\Delta p = 8$ bar and taking realistic figures for liquid Al this effect can be shown to be negligible¹⁰.

Finally, pore growth is also linked to coalescence. We observed that at low pressures the rate of coalescence is largely increased (see fig. 5). As this takes place at almost the same total volume of the foam, the average pore size must increase. Rupture therefore also contributes to an enhanced pore growth.

Therefore the pore size achieved under a certain pressure is the result of a complex interplay between different mechanisms.

4. Summary and Conclusions

Foamable precursors of AlSi6Cu4 + 0.5 wt% TiH₂ were prepared by uni-axial pressing. The samples were investigated by means of in-situ X-ray radiography in a X-ray transparent pressure furnace. Foam expansion, coalescence strength in the expanded state, pore size diameter and roundness were measured quantitatively under different gas pressures.

The expansion evolution was observed during the foaming process and a maximal foam expansion was found at around 3 – 5 bar. It could be shown that with increasing pressure foam stability increases, while collapse and coalescence phenomena are reduced.

The mean and the maximal pore diameter are clearly pressure dependent. They increase with decreasing pressure as well as foam homogeneity. Pore size versus pressure does not follow a simple ideal gas law. Other pressure-dependent effects such as decomposition of the blowing agent and increasing coalescence should contribute to the final structure. Pore roundness has a maximum at 7 – 8 bar, where the pores do not touch each other.

Metal foams with a given density and pore size can be produced at the same foaming temperature just by adjusting the surrounding gas pressure. This could be an interesting processing variant for industrial foam production.

Acknowledgments

This work was supported by the ESA-MAP-Program, grant MAP-99-075 and DFG, grant Ba1170 3-3.

REFERENCES

- 1) W. Seeliger, "Cellular Materials", eds. J. Banhart, N.A. Fleck, A. Mortensen, MIT-Verlag Berlin, 89, Berlin, June (2003) pp. 5-8
- 2) H. Stanzick, I. Duarte, J. Banhart, Mat.-wiss. u. Werkstoff. **31** (2000) pp. 409-411
- 3) F. Garcia-Moreno, J. Banhart, M. Haesche, K. Vignodhar, J. Weise: 1st Intern. Symposium on Cellular Metals for Structural and Functional Applications, Cellmet2005, Dresden, May (2005), in press.
- 4) F. Garcia-Moreno, N. Babcsan, J. Banhart, Coll. a. Surf. A **263** (2005) pp. 290-294

- 5) F. Simancik, N. Minarikova, S. Culak , J. Kovacik, *Proceedings to the Conference on Metal Foams and Porous Metal Structures, MetFoam 99*, Edited by J. Banhart, M.F. Ashby, N.A. Fleck, Bremen, June (1999) pp.105-108
- 6) C. Kömer, F. Berger, M. Arnold, C. Stadelmann, R.F. Singer, *Mat. Sci. and Techn.* **16** (2000) pp. 781-784
- 7) F. Garcia-Moreno, N. Babcan, J. Banhart, M. Haesche, J. Weise: *Proc. of the Symposium on Cellular Metals and Polymers*, ed. R.F. Singer et al., (Trans Tech Publications, 2005) pp. 31-34.
- 8) F. Garcia-Moreno, M. Fromme, J. Banhart, *Adv. Eng. Mater.* **6** (2004) pp. 416-420
- 9) Image Tool: <http://ddsdx.uthscsa.edu/dig/>
- 10) F. Garcia-Moreno, J. Banhart, to be published